Time-dependent effective behavior of jointed materials

Cássio B. Aguiar[1], Rodrigo Rossi[2], Samir Maghous[1]

[1]*Department of Civil Engineering, Federal University of Rio Grande do Sul*
Av. Osvaldo Aranha, 99, 90035-190 Porto Alegre-RS, Brazil
cassio.barros.aguiar@gmail.com, samir.maghous@ufrgs.br
[2]*Department of Mechanical Engineering, Federal University of Rio Grande do Sul*
Av. Osvaldo Aranha, 425, 90046-902 Porto Alegre-RS, Brazil
rrossi@ufrgs.br

Abstract. Inspections carried out on materials used in engineering often reveal the presence of discontinuities in different shapes and scales. Discontinuities are one of the main forms of physical-mechanical degradation of the material's properties. More specifically, joints are a particular type of discontinuity whose geometry is plane and have the mechanical capacity to transfer efforts along their opposite faces. Most works that aim to determine the properties of jointed materials tend to neglect differed deformation components, which are fundamental in several engineering fields. In this context, this work aims to propose a constitutive law that describes the effective behavior of viscoelastic jointed materials, without disregard aging effects. Backed by laboratory tests, the joints are modeled as interfaces whose mechanical behavior relates the stress vector to the displacement jumps on the joint's faces. Coupling the viscoelastic behavior of the constituents (solid matrix and joints) to micromechanical relationships, the homogenized creep tensor was analytically formulated, being written as the creep tensor of the solid matrix added to a fourth-order tensor related to the joints' properties. Classic cases of rock mechanics are derived, which show that particular distributions of joints families can cause anisotropy in the effective behavior of the material.

Keywords: Joints, Viscoelasticity, Micromechanics, Homogenization, Aging.

1 Introduction

It is well established from laboratory and in situ observations that engineering materials display at different scales discontinuity surfaces with various sizes and orientations. Ranging from the fine (crystalline) to large (geodetic) scale, these discontinuities are usually referred to as joints or fractures and correspond to thin layers along which the physical and mechanical properties of the intact solid matrix significantly degrade. Since joints exhibit much poorer mechanical properties than the intact material [1-3], their presence strongly affects the overall behavior of rock media and constitute an essential weak component for the material.

The viscoelastic behavior of jointed materials with long joints is frequently encountered in rock engineering problems [4-6]. The adjective 'long' refers to discontinuities that cut through the representative elementary volume of the material. In the modeling aspect, joints are viewed as 2D interfaces endowed with specific mechanical properties in normal and tangential directions. Provided that the rock medium involves a high density of long joint families, it appears advisable to resorts to the homogenized-based approaches and related micromechanical tools for the prediction of overall constitutive model of such materials [7].

The primary purpose of the present paper is to formulate the homogenized linear viscoelastic behavior of a jointed material from the knowledge of the joints and rock material respective properties. The three-dimensional formulation of the creep properties of the jointed rock is achieved by solving in the time domain a viscoelastic concentration problem stated on the representative elementary volume with prescribed stress loading history. The closed-form expressions do not require any restricting assumption regarding the joint orientations or associated constitutive model. An important feature of the homogenized model is related to its ability to cover a wide range of configurations while remaining simple to compute.

2 Modeling framework

The upscaling procedure developed in the subsequent analysis is based on micromechanical concepts, relying upon the concept of a representative elementary volume (REV) for densely jointed mediums. In this context, we assume it is possible to define a REV for the studied materials with randomly distributed joints. On the following reasoning Ω stands for the REV of homogeneous matrix material cut by a discrete distribution of N joint families $\omega = \bigcup_{j=1}^{N} \omega_j$ (Fig. 1) whereas the symbol $\Omega \backslash \omega$ refers to the homogeneous matrix material without the joints. Each joint family ω_j comprise a large number of same-orientation and mechanical-properties long joints crosscutting the REV. From the geometrical viewpoint, the joints are represented by flat planes, whose thickness and curvature can be neglected at the REV scale. The average spacing d^j of the jth joint family can be viewed as the characteristic dimension of the family [4] and should be very small with respect to the joint extension and to the size of the REV. At the REV scale, each joint is modeled from a constitutive mechanical viewpoint as an interface, geometrically described by a surface whose orientation is defined by a normal unit vector $\underline{n}^j$ (Fig. 1).

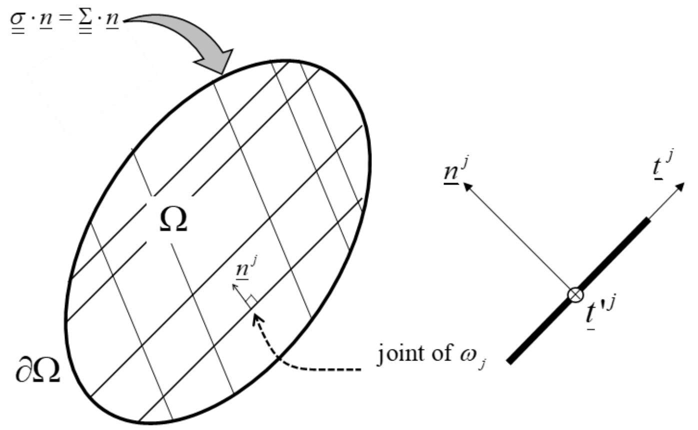

Figure 1. Representative elementary volume of the jointed material and associated loading mode conditions.

The matrix material is modeled as a 3D continuum. The displacement field $\underline{\xi}$, strain field $\underline{\underline{\varepsilon}}$ and stress field $\underline{\underline{\sigma}}$ are defined as usually on $\Omega \backslash \omega$. In that respect, the symbol $\langle \bullet \rangle$ refers to the average operator over the matrix material domain:

$$\langle \bullet \rangle = \frac{1}{\Omega} \int_{\Omega \backslash \omega} \bullet \, dV \tag{1}$$

The counterpart fields for a joint of family ω_j, are the displacement jump $[\underline{\xi}]$ across the joint when following its normal $\underline{n}^j$, and the stress vector $\underline{T} = \underline{\underline{\sigma}} \cdot \underline{n}^j$ acting upon the joint interface. The mechanical load applied to the REV corresponds to prescribed homogeneous stress boundary conditions [7]

$$\underline{\underline{\sigma}}(\underline{x}) \cdot \underline{n}(\underline{x}) = \underline{\underline{\Sigma}} \cdot \underline{n}(\underline{x}) \quad \forall \underline{x} \in \partial\Omega \tag{2}$$

where $\underline{n}(\underline{x})$ is the outer unit normal vector to the VER boundary $\partial\Omega$ at any point $\underline{x} \in \partial\Omega$ and $\underline{\underline{\Sigma}}$ represents the applied macroscopic stress tensor. For any statically admissible stress field $\underline{\underline{\sigma}}$, that is, satisfying the momentum balance equation $\operatorname{div} \underline{\underline{\sigma}} = 0$, the continuity of stress vector $\underline{T} = \underline{\underline{\sigma}} \cdot \underline{n}^j$ when crossing any joints of family ω_j and complying with the boundary condition (2) , it can be established from a classical reasoning that:

$$\underline{\underline{\Sigma}} = \langle \underline{\underline{\sigma}}(\underline{x}) \rangle \tag{3}$$

Making use of the generalized form of Hill's lemma [5-6], the macroscopic strain of jointed medium can be written as the contribution of two components by means of

$$\underline{\underline{\mathrm{E}}} = \langle \underline{\underline{\varepsilon}} \rangle + \frac{1}{\Omega} \int_{\omega} \underline{n} \overset{s}{\otimes} [\underline{\xi}] \, dS \tag{4}$$

Where the first contribution $\langle \underline{\underline{\varepsilon}} \rangle$ refers to the matrix average strain whereas the second term is related to the joints average deformation. The operator $\overset{s}{\otimes}$ stands for the symmetric part of dyadic product: $(\underline{u} \overset{s}{\otimes} \underline{v})_{ij} = (u_i v_j + v_i u_j)/2$ in terms of components with respect to an orthonormal base.

3 Effective viscoelastic behavior of the jointed medium

The viscoelastic formulation developed in this paper was concerned as an extension of Maghous and coauthors' model [5], formulated within the framework of infinitesimal linear elasticity. Even so, the present work gives up the concept of non-linearity (present in [5]) associated with the elastic behavior of the rock matrix and joints. In the context of infinitesimal strain analysis, the stress-strain viscoelastic relationship for solids reads

$$\underline{\underline{\varepsilon}}(t) = \mathbb{F}^s \odot \underline{\underline{\sigma}} = \mathbb{F}^s(t,t) : \underline{\underline{\sigma}}(t) + \int_0^t \frac{\partial \mathbb{F}^s}{\partial \tau}(\mathrm{t},\tau) : \underline{\underline{\sigma}}(\tau) d\tau \tag{5}$$

where $\mathbb{F}^s$ stands for the fourth-order creep tensor associated with rock matrix behavior and the operator $\odot$ define the Boltzmann hereditary integral. This relationship relates the local stress and strain fields at any point of the domain $\Omega \setminus \omega$.

Before introducing the viscoelastic behavior of the joints, it is convenient to express the elastic behavior of the joints, relating the stress vector to the displacement jump. It is assumed that any element of the family ω_j is characterized by the joint stiffness $\underline{\underline{k}}^j$ relating the displacement jump $\left[\underline{\xi}\right]$ to the stress vector $\underline{T}$ through

$$\underline{T} = \underline{\underline{k}}^j \cdot [\underline{\xi}] \quad \text{or} \quad [\underline{\xi}] = \underline{\underline{s}}^j \cdot \underline{T} \tag{6}$$

where $\underline{\underline{s}}^j$ is the second-order compliance tensor of the joints of family ω_j. The joint stiffness $\underline{\underline{k}}^j$ (or alternatively the joint compliance $\underline{\underline{s}}^j$) is classically evaluated from appropriate laboratory tests carried out on jointed specimens. The works of Goodman [1] and Bandis and coauthors [2] represent reference contributions regarding the experimental identification of elastic joint properties.

In the context of this work, the relationship between the stress vector and the displacement jump is extended to the viscoelastic framework by means of the following formulation

$$[\underline{\xi}](t) = \underline{\underline{F}}^j \odot \underline{T} = \underline{\underline{F}}^j(t,t) \cdot \underline{T}(t) + \int_0^t \frac{\partial \underline{\underline{F}}^j}{\partial \tau}(\mathrm{t},\tau) \cdot \underline{T}(\tau) d\tau \tag{7}$$

where $\underline{\underline{F}}^j$ stands for the second-order creep tensor associated to the jth joint family behavior. The operator $\odot$ can be viewed as a second-order Boltzmann hereditary integral. Considering the orthonormal local frame $(\underline{n}^j, \underline{t}^j, \underline{t}'^j)$ (Fig. 1), defined for each joint of the set ω_j by the unit normal vector $\underline{n}^j$ and by two orthogonal unit vectors $(\underline{t}^j, \underline{t}'^j)$ of the plane parallel to joint direction, the components of $\underline{\underline{F}}^j$, disregarding the coupling between joint normal and shear behavior, reads

$$\underline{\underline{F}}^j = F_n^j \ \underline{n}^j \otimes \underline{n}^j + F_t^j \ \underline{t}^j \otimes \underline{t}^j + F_{t'}^j \ \underline{t}'^j \otimes \underline{t}'^j \tag{8}$$

The creep function F_n^j stands for the joint creep function in normal direction, relating the normal displacement jump $[\underline{\xi}] \cdot \underline{n}$ to the normal stress $\sigma_n = \underline{T} \cdot \underline{n}^j$. Component F_t^j (resp. $F_{t'}^j$) is the tangential creep function, relating the displacement jump $[\underline{\xi}] \cdot \underline{t}$ (resp. $[\underline{\xi}] \cdot \underline{t}'$) to the shear stress $\sigma_t = \underline{T} \cdot \underline{t}^j$ (resp. $\sigma_{t'} = \underline{T} \cdot \underline{t}'$). Appropriate creep tests are necessary to assess the joint creep functions F_n^j, F_t^j and $F_{t'}^j$ [3].

Given the prescribed macroscopic stress history $\underline{\underline{\Sigma}}(\tau)$, the formulation of the effective viscoelastic behavior in the following upscaling problem requires solving $(\underline{\underline{\sigma}}, \underline{\xi})$ satisfying at any instant $t \geq 0$ the following conditions

$$\begin{cases} \operatorname{div} \underline{\underline{\sigma}} = 0 & (\Omega \backslash \omega) \\ \underline{T} = \underline{\underline{\sigma}} \cdot \underline{n}^j \text{ is continous when crossing } \omega_j & \\ \underline{\underline{\sigma}} \cdot \underline{n} = \underline{\underline{\Sigma}} \cdot \underline{n} & (\partial \Omega) \\ \underline{\underline{\varepsilon}} = \mathbb{F}^s \odot \underline{\underline{\sigma}} & (\Omega \backslash \omega) \\ [\underline{\xi}] = \underline{\underline{F}}^j \odot \underline{T} & (\omega_j) \end{cases} \tag{9}$$

Similarly to the elastic upscaling problem [5], the viscoelastic concentration problem (Eq.(9)) admits the following homogeneous stress solution

$$\underline{\underline{\sigma}}(\underline{x}, t) = \underline{\underline{\Sigma}}(t) \quad \forall \underline{x} \in \Omega \setminus \omega \tag{10}$$

The strain average rule (Eq.(4)) together with the constitutive viscoelastic equations (Eq. (5) and Eq. (7)) and the homogeneous solution (Eq. (10)) allow computing the macroscopic strain as

$$\underline{\underline{\mathrm{E}}} = \mathbb{F}^s(t,\tau) \odot \underline{\underline{\Sigma}} + \sum_{j=1}^N a^j \left(\underline{\underline{F}}^j \odot \underline{\underline{\Sigma}} \cdot \underline{n}^j \right) \overset{s}{\otimes} \underline{n}^j \tag{11}$$

where $a^j = 1/\Omega \int_{\omega_j} dS$ is the specific area of the joint family ω_j, which could be evaluated by the inverse of average joint spacing value. Equation (11) can be rearranged as

$$\underline{\underline{E}} = \mathbb{F}^{\text{hom}} \odot \underline{\underline{\Sigma}} \tag{12}$$

which implies that the expression of homogenized creep tensor $\mathbb{F}^{\text{hom}}$ reads

$$\mathbb{F}^{\text{hom}} = \mathbb{F}^s(t,\tau) + \sum_{j=1}^{N} \mathbb{F}^j(t,\tau) \tag{13}$$

with

$$\mathbb{F}^j = a^j \left(F_n^1 \underline{n}^j \otimes \underline{n}^j \otimes \underline{n}^j \otimes \underline{n}^j + F_t^j \underline{t}^j \overset{s}{\otimes} \underline{n}^j \otimes \underline{t}^j \overset{s}{\otimes} \underline{n}^j + F_{t'}^j \underline{t}'^j \overset{s}{\otimes} \underline{n}^j \otimes \underline{t}'^j \overset{s}{\otimes} \underline{n}^j \right) \tag{14}$$

According Eq. (13), some important conclusions are achieved:

- In addition to the original constituent's anisotropy, a strong anisotropy of the macroscopic viscoelastic properties shall be associated with the privileged joint orientations.
- The overall creep properties are obtained by adding separately the individual contributions of the rock matrix and of each joint family. This feature is attributed to the assumption of homogeneity for the rock matrix and to the modeling of joints as infinite planar interfaces
- The aging properties from matrix material and joints are integrally transposed to the macroscopic scale. In addition to explaining the existence of aging in the effective behavior of the material, it can be observed that the intensity of aging is linked to the aging of materials in the microscale.

4 Particular solution: Effective behavior with two families of joints

This section aims to present the particular solution of Eq. (13) configured by a solid matrix intersected by two joint families ω_1 and ω_2. The relative angular inclination between the corresponding joint normal directions is denoted by θ (Fig. 2). The explicit calculation of $\mathbb{F}^{\text{hom}}$ will be achieved by expressing its components in the fixed frame $(\underline{e}_1, \underline{e}_2, \underline{e}_3) = (\underline{n}^1, \underline{t}^1, \underline{t}'^1)$ attached to the joints of family ω_1, choosing the unit vector $\underline{e}_3$ parallel to the direction defined by the intersection line between a joint of ω_1 and a joint of ω_2. The general expression of $\mathbb{F}^{\text{hom}}$ is reduced in the particular situation of two sets of families to

$$\begin{aligned}\mathbb{F}^{\text{hom}} = \mathbb{F}^s + a^1 &\left(F_n^1\, \underline{e}_1 \otimes \underline{e}_1 \otimes \underline{e}_1 \otimes \underline{e}_1 + F_t^1\, \underline{e}_2 \overset{s}{\otimes} \underline{e}_1 \otimes \underline{e}_2 \overset{s}{\otimes} \underline{e}_1 + F_{t'}^1\, \underline{e}_3 \overset{s}{\otimes} \underline{e}_1 \otimes \underline{e}_3 \overset{s}{\otimes} \underline{e}_1 \right) \\ a^2 &\left(F_n^2\, \underline{n}^2 \otimes \underline{n}^2 \otimes \underline{n}^2 \otimes \underline{n}^2 + F_t^2\, \underline{t}^2 \overset{s}{\otimes} \underline{n}^2 \otimes \underline{t}^2 \overset{s}{\otimes} \underline{n}^2 + F_{t'}^2\, \underline{t}'^2 \overset{s}{\otimes} \underline{n}^2 \otimes \underline{t}'^2 \overset{s}{\otimes} \underline{n}^2 \right)\end{aligned} \tag{15}$$

where the vectors $\underline{n}^2$, $\underline{t}^2$ and $\underline{t}'^2$ define the contribution of ω_2 joint family , which are expressed in the reference frame $(\underline{e}_1, \underline{e}_2, \underline{e}_3)$ by means of the angle θ

$$\underline{n}^2 = \cos\theta\, \underline{e}_1 - \sin\theta\, \underline{e}_2 \quad ; \quad \underline{t}^2 = \sin\theta\, \underline{e}_1 + \cos\theta\, \underline{e}_2 \quad ; \quad \underline{t}'^2 = \underline{e}_3 \tag{16}$$

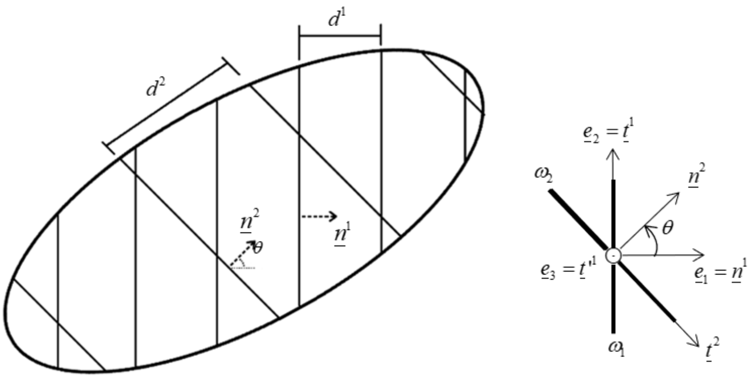

Figure 2. Matrix material cut by two families of joints: REV and reference frame.

Assuming isotropic viscoelastic properties to the solid matrix, the associated creep tensor $\mathbb{F}^s$ can conveniently be expressed as

$$\mathbb{F}^s = \frac{1}{3} F_k^s \; \mathbb{J} + \frac{1}{2} F_\mu^s \; \mathbb{K} \tag{17}$$

where F_k^s and F_μ^s are respectively the creep function in bulk and the creep function in shear of the solid matrix. The fourth-order tensors $\mathbb{J}$ and $\mathbb{K}$ are defined as $\mathbb{J} = 1/3 \; \underline{\underline{1}} \otimes \underline{\underline{1}}$ and $\mathbb{K} = \mathbb{I} - \mathbb{J}$.

Conveniently, it is possible write the fourth-order homogenized creep tensor by means of the following matrixial representation

$$\mathbb{F}^{\text{hom}} \equiv \begin{bmatrix} \frac{F_k^s}{9} + \frac{F_\mu^s}{3} + \alpha_{11} & \frac{F_k^s}{9} - \frac{F_\mu^s}{6} + \alpha_{12} & \frac{F_k^s}{9} - \frac{F_\mu^s}{6} & 0 & 0 & \alpha_{16} \\ \frac{F_k^s}{9} - \frac{F_\mu^s}{6} + \alpha_{12} & \frac{F_k^s}{9} + \frac{F_\mu^s}{3} + \alpha_{22} & \frac{F_k^s}{9} - \frac{F_\mu^s}{6} & 0 & 0 & \alpha_{26} \\ \frac{F_k^s}{9} - \frac{F_\mu^s}{6} & \frac{F_k^s}{9} - \frac{F_\mu^s}{6} & \frac{F_k^s}{9} + \frac{F_\mu^s}{3} & 0 & 0 & 0 \\ 0 & 0 & 0 & F_\mu^s + \alpha_{44} & \alpha_{45} & 0 \\ 0 & 0 & 0 & \alpha_{45} & F_\mu^s + \alpha_{55} & 0 \\ \alpha_{16} & \alpha_{26} & 0 & 0 & 0 & F_\mu^s + \alpha_{66} \end{bmatrix} \tag{18}$$

where the non-null terms corresponding to the joints contribution are

$$\begin{cases} \alpha_{11} = a^1 F_n^1 + a^2 \left[F_n^2 \cos^4\theta + \frac{1}{4} F_t^2 \sin^2 2\theta \right] \; ; \quad \alpha_{22} = a^2 \left[F_n^2 \sin^4\theta + \frac{1}{4} F_t^2 \sin^2 2\theta \right] \\ \alpha_{44} = a^2 F_{t'}^2 \sin^2\theta \; ; \quad \alpha_{55} = a^1 F_{t'}^1 + a^2 F_{t'}^2 \cos^2\theta \\ \alpha_{66} = a^1 F_t^1 + a^2 \left[F_n^2 \sin^2 2\theta + F_t^2 \cos^2 2\theta \right] \; ; \quad \alpha_{12} = a^2 \left[\frac{1}{4} F_n^2 \sin^2 2\theta - \frac{1}{4} F_t^2 \sin^2 2\theta \right] \\ \alpha_{16} = a^2 \left[-F_n^2 \cos^2\theta \sin 2\theta + \frac{1}{4} F_t^2 \sin 4\theta \right] \\ \alpha_{26} = a^2 \left[-F_n^2 \sin^2\theta \sin 2\theta - \frac{1}{4} F_t^2 \sin 4\theta \right] \; ; \quad \alpha_{45} = a^2 \frac{1}{2} F_{t'}^2 \sin 2\theta \end{cases} \tag{19}$$

It is noted that the above representation is consistent with the following matrix notation for stress and strain

$$\underline{\underline{\sigma}} \equiv {}^T\left[\; \sigma_{11} \;\; \sigma_{22} \;\; \sigma_{33} \;\; \sigma_{23} \;\; \sigma_{13} \;\; \sigma_{12} \; \right] \quad ; \quad \underline{\underline{\varepsilon}} \equiv {}^T\left[\; \varepsilon_{11} \;\; \varepsilon_{22} \;\; \varepsilon_{33} \;\; 2\varepsilon_{23} \;\; 2\varepsilon_{13} \;\; 2\varepsilon_{12} \; \right] \tag{20}$$

where subscript $'T'$ stands for the transposition of a vector.

5 Example of application

We examine in this section the overall creep properties in shear of a shale rock cut by a single family of crosscutting joints as schematized in Fig. 3. The particular solution of this example could be accessed using Eq.(15) doing $F_n^2 = 0$, $F_t^2 = 0$ and $F_{t'}^2 = 0$. Subscript $'j'$ referring to joints is omitted in this section. By sake of simplicity, the aging effect will not be analyzed in this section.

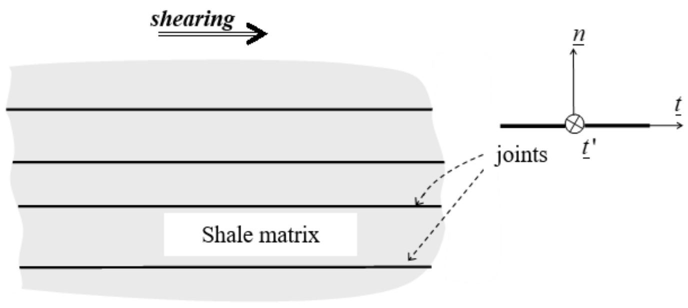

Figure 3. Shale-like rock under shearing parallel to joints direction.

Based on viscoelastic shear creep experimental data ([3] and [8]), the individual non-aging viscoelastic behavior in shear of the shale rock matrix (Fig. 6-a) and of the joints (Fig. 6-b) can be modeled according the rheological Kelvin-Voigt models.

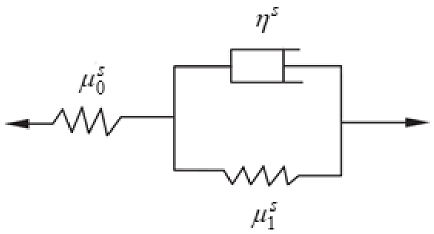

(a) viscoelastic shear model $\mu^s(t)$ for matrix material

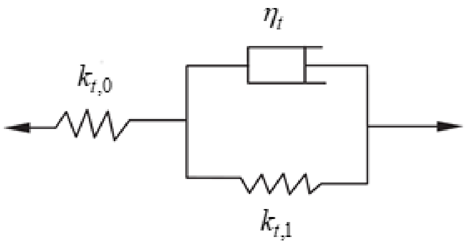

(b) viscoelastic shear model $k_t(t)$ for joints

Figure 4. Kelvin-Voigt rheological models used for the constituents of the jointed rock.

The values of the parameters defining the shear relaxation modulus of the shale matrix $\mu^s(t)$ and that of the joints $k_t(t)$ provided in the above mentioned works are

Table 1. Material parameters defining the shear behavior of the matrix and of the joints.

$\mu_0^s = 0.181$ GPa	$\mu_1^s = 0.299$ GPa	$\eta^s = 7.539$ GPa.h
$k_{t,0} = 6.338$ GPa/m	$k_{t,1} = 5.333$ GPa/m	$\eta_t = 5.792$ GPa.h/m

Assuming isotropy for the joint shear response (i.e., $k_{t'} = k_t$), the shear creep component reads therefore

$$F_{shear}^{\text{hom}} = F_\mu^s + a\,F_t \quad (21)$$

where the creep functions F_μ^s and F_t of the rock matrix and the joints are obtained from the relaxation counterparts μ^s and k_t (associated with the respective Kelvin-Voigt models) by inverse Boltzmann operator.

Taking a joint specific area equal to $a = 10\ \text{m}^{-1}$, corresponding to an average joint spacing of $0.1\ \text{m}$, Fig. 5 displays temporal evolution of the homogenized creep function in shear comparing to the intact shale rock.

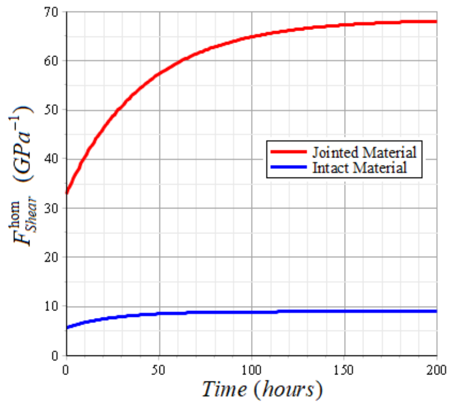

Figure 5. Time evolution of the shear creep functions of the intact and jointed rocks.

Figure 5 exhibit the significant increase in the shear creep function induced by the presence of the joints when compared to that of the intact material. This result is corroborating laboratory observations over high joint density rocks, such as shale-like rocks, which proves the time-dependent properties are strongly affected by the presence of discontinuities, which increase the overall deformability of the rock mass [8]. Additionally, the joints properties affect mainly the early stages ($t < 100\ \text{h}$) of homogenized creep function, increasing significantly the evolution rate. Although only the component associated with shearing parallel to the joints was analyzed, similar observations could be expected for the other components of the overall creep components.

6 Conclusions

Relying upon an upscaling approach developed in the context of micromechanics of randomly heterogeneous materials, the effective viscoelastic properties of a jointed material have been assessed. The formulation explicitly addresses the situation of materials with a dense network of crosscutting joints and extends early formulations to aging linear viscoelasticity. In the framework of modeling, the joints are viewed as planar interfaces whose constitutive behavior relates the local stress vector and displacement jump histories.

The micromechanical reasoning consisted in solving the viscoelastic concentration problem stated on the representative elementary volume of the jointed material. General closed-form expressions for the homogenized creep properties have been thereby derived from the knowledge of the viscoelastic behavior of the individual constituents. The creep anisotropy induced by the existence of the privileged directions associated with the joint orientation distribution is automatically accounted for in the homogenization process. An important feature of the formulation lies on the fact that the overall creep tensor expresses as the sum of the individual contributions of solid matrix and each joint family, thus disregarding the possible interaction between the joint's family. This is clearly attributed to the assumed homogeneity of rock matrix at the REV scale and the modeling of the joints as infinite planar interfaces.

It should be emphasized that effective validation of the theoretical modeling remains to be achieved through comparison of the model predictions against experimental data from laboratory or field tests. In that respect, a major concern is the lack in available data regarding the creep properties of joints. A possible strategy to overcome this difficulty could rely upon inverse analyses developed at macroscopic scale with the aim to identify the viscoelastic properties of the constituents (i.e., solid matrix and joints) from direct comparisons with experimental results referring to the material or structure levels.

Acknowledgements. The authors gratefully appreciate the support provided by the Brazilian Research Council (CNPq) and the Federal University of Rio Grande do Sul (UFRGS).

Authorship statement. The authors hereby confirm that they are the sole liable persons responsible for the authorship of this work, and that all material that has been herein included as part of the present paper is either the property (and authorship) of the authors, or has the permission of the owners to be included here.

References

[1] R.E. Goodman, *Methods of geological engineering in discontinuous rocks*. West Publishers, St Paul ,1976.
[2] C.S. Bandis, A.C. Lumsden and N.R. Barton, "Fundamentals of rock joint deformation". *International Journal of Rock Mechanics and Mining Sciences & Geomechanics Abstracts*. vol. 20, pp. 249-268, 1983
[3] S.Q. Yang and L. Cheng, "Non-stationary and nonlinear visco-elastic shear creep model for shale". *International Journal of Rock Mechanics & Mining Sciences*. vol. 48, pp. 1011-1020, 2011.
[4] S. Maghous, P. de Buhan, L. Dormieux and D. Garnier, "Macroscopic elastoplastic behaviour of a jointed rock medium". *Comptes rendus de l'Académie des Sciences*. vol. 328(IIb), pp. 701-708, 2000
[5] S. Maghous, D. Bernaud, J. Fréard and D. Garnier, "Elastoplastic behavior of jointed rock masses as homogenized media and finite element analysis". *International Journal of Rock Mechanics & Mining Sciences*. vol. 45, pp. 1273-1286, 2008.
[6] S. Maghous, L. Dormieux, D. Kondo and J. F. Shao, "Micromechanics approach to poroelastic behavior of a jointed rock". *International Journal for Numerical and Analytical Methods in Geomechanics*, vol. 37, pp. 111-129, 2013.
[7] A. Zaoui, "Continuum micromechanics: a survey". *Journal of Engineering Mechanics ASCE*. vol. 128, pp. 808-816, 2002.
[8] H.-P. Chin and J. D. Rogers, "Creep parameters of rocks on an engineering scale". *Rock Mechanics and Rock Engineering volume*. vol. 20, pp. 137-146, 1987.